Received: 26 September 2016 | Revised: 26 February 2017 | Accepted: 28 March 2017

DOI: 10.1002/cem.2907

RESEARCH ARTICLE

WILEY Journal of CHEMOMETRICS

Intelligent tools to model photocatalytic degradation of beta-naphtol by titanium dioxide nanoparticles

Hossein Ijadpanah-Saravi[1] | Mehdi Safari[2] | Behrooz Noruzi-Masir[3] | Ahmad Khodadadi Darban[4] | Puyan Bakhshi[3]

[1] Concordia University, Montreal, Quebec, Canada

[2] University of Kurdistan Hewler (UKH), Kurdistan, Iraq

[3] Peroleum University of Technology, Ahwaz, Iran

[4] Tarbiat Modares University, Tehran, Iran

Correspondence
Behrooz Noruzi-Masir, Petroleum Department, Petroleum University of Technology, 6198144471, Ahwaz, Iran.
Email: b.noruzi88@yahoo.com

Feasibility of applying intelligent tools in prediction and optimization of photocatalytic degradation of beta-naphthol using the titanium dioxide (TiO_2) nanoparticles were conducted in this study. Biphasic TiO_2 nanoparticles were synthesized using the controlled hydrolysis of $TiCl_4$, and their properties were studied using the X-ray diffraction and transmission electron microscopy methods. Therefore, factors affecting photocatalytic degradation of beta-naphthol including impurity concentration, catalyst content, acidity, and aeration rate were monitored and controlled. The laboratory data showed that degradation rate of beta-naphthol is a complicated nonlinear function of monitored variables. Two models including artificial network trained with particle swarm optimization (ANN-PSO) and adaptive neuro-fuzzy interference system trained with particle swarm optimization (ANFIS-PSO) were used for prediction of this system. The results showed presence of a significant relation between the real and predicted data of these 2 models. However, ANFIS-PSO can be more efficiently applied for prediction and optimization of photocatalytic behavior of TiO_2 nanoparticles as for degradation of beta-naphthol as compared to ANN-PSO. As an advantage, ANFIS eliminates the problems of fuzzy logic, such as creation of membership functions, and local minima, which should be located in design of ANN, and through PSO algorithm, it could be a very powerful tool for simulating kinds of processes.

KEYWORDS
artificial neural network, beta-naphthol photodegradation, neuro-fuzzy system, swarm optimization, TiO_2 nanoparticles

1 | INTRODUCTION

By the ever-increasing advances in the new wastewater treatment processes, photocatalytic processes have found a wide application in treatment of toxic and nondegradable contaminations.[1] Through these processes, contamination concentration drops from several hundred mgr/lit below 10 mgr/lit within a short time.[2] Molecules of a photocatalyst such as titania are excited by energy absorption from high-energy UV photons and transferred to the conductance layer. Such a shift creates a hole in valance layer and an electron in conductance layer. These sites generate hydroxide and superoxide radicals by adsorbing H_2O and O_2 molecules, respectively. These radicals degrade the contaminator molecules in the solution by invading them. Next, through the photocatalytic reactions, the organic molecules of the contaminator molecule are degraded to CO_2 and H_2O.[2,3] As a member of poly ring aromatic hydrocarbons family, beta-naphthol is found in waste water of various factories producing chemicals such as pesticides, oil refineries, and

petrochemical factories. Photocatalytic degradation of beta-naphthol using the TiO_2 nanoparticles is controlled using various factors such as catalyst content, concentration of beta-naphthol, aeration rate, and acidity,[4] where a change in any of these factors affects the beta-naphthol degradation rate.

In this study, artificial intelligence techniques, which are among the most current approaches for prediction and processing of engineering data, are applied to predict beta-naphthol degradation by the controlling factors. Artificial intelligence tools have a flexible mathematical structure, which is able to extract the complicated nonlinear relations among the input and output data. In this work, 2 models including artificial network trained with particle swarm optimization (ANN-PSO) and adaptive neuro-fuzzy interference system trained with particle swarm optimization (ANFIS-PSO) were used for prediction and modeling performance of the biphasic nano-TiO_2. The artificial intelligence models are trained using the laboratory and recorded data, where they are informed of the relationship between the independent input variables and the output variable.[5,6] Recently, artificial intelligence has been frequently used as a simple versatile method for analysis of nonlinear problems in various fields of environmental engineering.[7-9] Among the frequent application of artificial intelligence, one can name prediction of chlorine concentration in urban water,[10,11] determination of qualitative relationships of waste water,[12,13] salinity and thermal modeling of the rivers and lakes, etc.[14,15]

Considering the novelty of photocatalytic processes, as a powerful tool for analysis of the linear and nonlinear relations among various variables, artificial intelligence has been recently applied for predicting the trend of these processes.[16-20] Using the artificial intelligence models allows lowering the costs and time needed by other modeling processes. Hence, to predict beta-naphthol degradation, this study was conducted to develop an artificial intelligence model and then apply the PSO algorithm. Accordingly, ANN and ANFIS were used for modeling and prediction of the mentioned process, and PSO algorithm was employed to optimize the parameters of these 2 methods.

The main goal pursued in this research is to extract the reasonable relationship among the effective parameters of the process such as concentration of contaminants, catalyst content, acidity, and aeration rate using the controlling factors of photocatalytic process. In this regard, 2 models with suitable architecture were developed for prediction and optimization of photocatalytic degradation of beta-naphthol.

2 | LABORATORY DATA

2.1 | Materials and methods

All chemicals used in this work were selected among the materials with high purity. Beta-naphthol, titanium tetrachloride, hydrochloric acid, and sodium hydroxide were purchased from Merck, Germany. Nano-TiO_2 particles were synthesized using the controlled hydrolysis of $TiCl_4$.[21] To synthesize titanium nanoparticles with a crystalline anatase form, 0.025 M ammonium sulfate was added slowly to 3-M TiCl4 to reach a concentration of 0.5 M. A 2.5-M ammonium hydroxide solution was added until the pH was 7. To synthesize the crystalline form of rutile, 0.5-M HCl was gradually added to 3-M TiCl4 to reach a concentration level of 0.5 M. To simultaneously synthesize both phases, a small amount of ammonium sulfate was added to the 3-M TiCl4. The final 0.5-M concentration was obtained after the addition of distilled water. To complete the hydrolysis, the solutions were heated to 70°C for 10 hours and gently stirred. To perform a homogenous hydrolysis process and avoid product heterogeneity (induced by direct admixture of the reagents), it was required to perform the steps slowly.[22,23] After completing the hydrolysis process, the synthesized powder was centrifuged and washed twice with distilled water. To prevent gel pore destruction and hard agglomeration between nanoparticles induced by the ordinary drying methods, an advanced superelectrical technique was used.[22,24] Finally, the samples were calcinated at 400°C for 2.5 hours. Detection of crystalline phases was performed using the X-ray diffraction (XRD) analysis (X'pert, 1480, Philips, Netherland). Also, study of the synthesized particles was performed using the transmission electron microscopy (TEM, model: EM10C 80 KV, Zeiss). Figure 1 illustrates XRD pattern and TEM image of the produced nanoparticles. Figure 1 presents that the produced nanoparticles have an average diameter of 18 to 22 nm. As well, the TEM micrograph confirms that produced nanoparticles are fully separated. The average particle size measured by TEM and XRD analysis was match together.

To determine the concentration of the organic volatile complex compounds, Agilent 6890 gas chromatograph (GC) was used. To inject the samples to the GC device, the analyzed material was transferred from the aqueous phase to the organic phase. To do so, first, 10 mL of the sample was mixed with 2 mL of dichloromethane and agitated for 1.5 hours. Once the agitation process is stopped, dichloromethane is deposited and segregated because it is heavier. The process was repeated twice more. Then, 6 mL of dichloromethane containing β-naphthol was heated at a mild temperature, and the mix volume was reduced to 1 mL.[22]

Finally, 1 μL of the mix was injected to the GC device. Thermal adjustment was performed in the following manner, where the oven temperature was kept at 65°C for 1 minute and then it was increased to 210°C with gradient of 15°C/min and kept at this temperature for 3 minutes. The injector and detector temperatures were adjusted in split less state at 200°C and 210°C, respectively.[22]

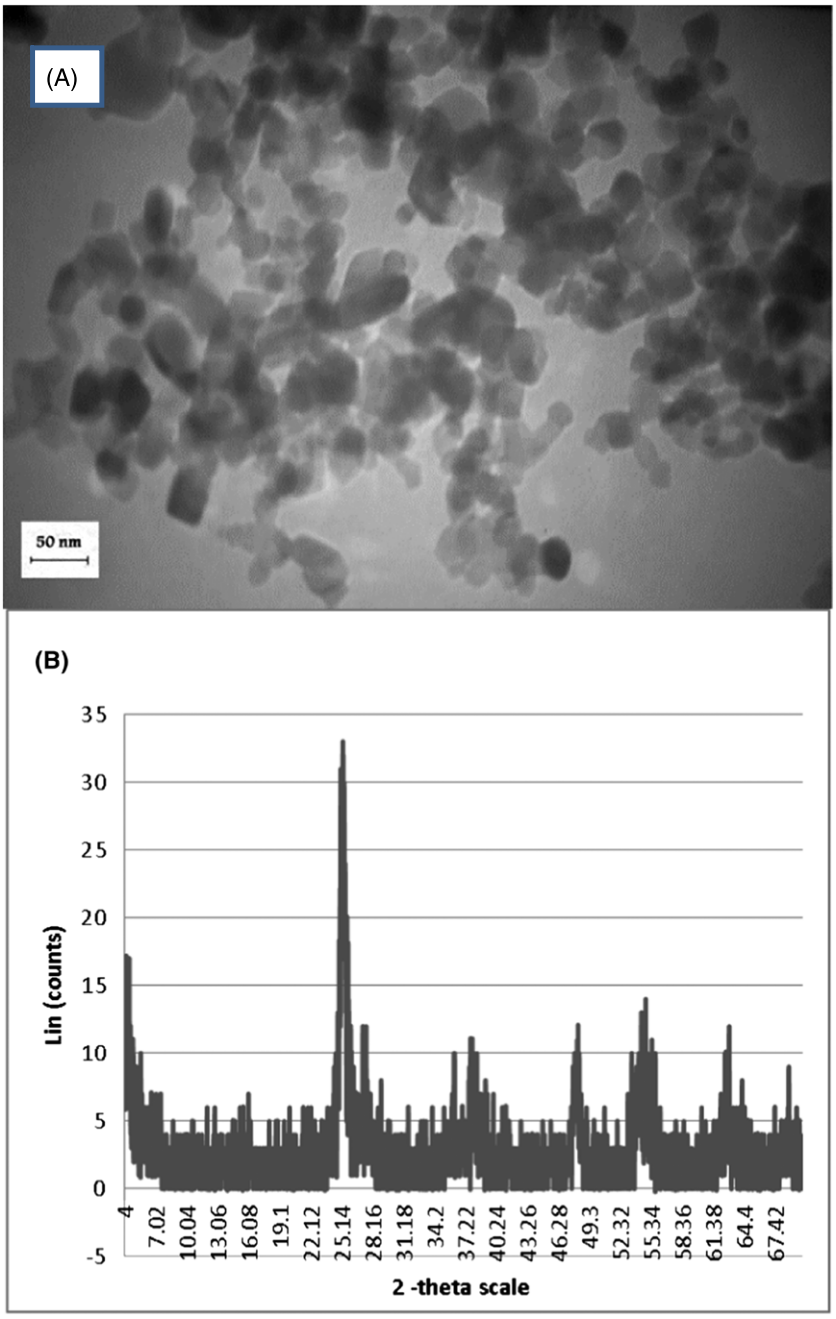

FIGURE 1 A, transmission electron microscopy micrograph; B, X-ray diffraction pattern of the produced nanoparticles

3 | MODELS DEVELOPED FOR PREDICTING THE APPLICATION OF BIPHASIC NANO-TIO_2 ON B-NAPHTHOL PHOTODEGRADATION

Artificial neural networks (ANNs) are learning machines, which undergo training processes by receiving some information. When training is completed, a validation step for network is started. Artificial neural network functions by constructing a nonlinear mapping between inputs and outputs and then converting these complex relationships to sequences of input-output training patterns. Therefore, to model complex and nonlinear systems where mathematical modeling might be deemed too complicated or unacceptable, this method can greatly be of use.[25,26] An ANN typically consists of a branch of a large number of nodes or neurons, which are arranged to form layers. Such layers are divided to 3 categories, ie, input layer, hidden layers, and output layer. In addition, ANNs contain weights for interconnecting the nodes of successive layers.[25-29] As the signal is carried from one node to the other, the mentioned weights will be modified, in the course of an iterative process, which uses an algorithm called training algorithm. Among the typically used training algorithms, the Back-Propagation (BP) algorithm is used the most. This algorithm is used with the aim of obtaining a set of the network weights for minimizing an error function. The most commonly used error function,

namely, the mean squared error (MSE), is defined as follows:

$$\mathrm{MSE} = \frac{1}{\mathrm{G}+\mathrm{m}} \sum_{\mathrm{k}=1}^{\mathrm{G}} \sum_{\mathrm{j}=1}^{\mathrm{m}} \left[\mathrm{Y_j(k)} - \mathrm{T_j(k)}\right]^2, \quad (1)$$

where m stands for the number of output nodes, G represents the number of training samples, $Y_j(k)$ is the expected output, and $T_j(k)$ is the actual output.

Artificial neural network has recently been used for modeling various processes[30-34]; though designing and training ANNs pose several problems. One of the most challenging problems is faced when one is assigning and defining weights for designing the network. Assignment of weights is a parameter affecting the performance of an ANN structure. The weights can be controlled by learning algorithm parameters and network structure. In a nutshell, further parameters, namely, the number of hidden layers, number of neurons in layers, and learning rates, could impact the performance of an artificial neural network structure. Because of the undisputable importance of ascertaining the network structure and parameters, some modern algorithms such as Particle Swarm Optimization, Back Propagation, Simulated Annealing, Genetic Algorithm, etc and traditional algorithms have been used on this account. Nonetheless, the above mentioned algorithms suffer certain disadvantages, for instance, the unpredictability and prematurity of the results obtained by Genetic Algorithm (GA) and the slow convergence speed of BP. Moreover, traditional methods are useful in finding the optimum solution of the functions that are continuous and differentiable. Traditional methods are classified into 2 categories: direct methods such as Bracketing and gradient methods such as Newton-Raphson. While the former methods do not use any derivative information of the objective function used to guide the search process, the latter ones use derivative information.[35] In general, while solving the problem of finding the optimum solution, nondifferentiable functions as well as differentiable ones may be faced. Consequently, traditional methods are not applicable for finding the optimum solutions for functions, which are discontinuous and/or nondifferentiable. Hence for a more general approach to tackle this problem, other algorithms are required for being applied in nonanalytical problems. Accordingly, finding a highly efficient algorithm has been one of the most important challenges in ANN application. For instance, Tahmasebi and Hezarkhani[32] optimized the parameters of ANN by using GA, and Samanta et al[36] used simulated annealing to design the structure of ANN.

Back-Propagation algorithm uses a searching strategy for optimal solutions along the direction of the maximum gradient descent. To prevent trapping in the local minima, which prolongs the convergence, GA uses stochastic searching strategy. In addition, this algorithm helps ANN to seek out the accurate solution and converge on the global minima more quickly.[37] Bahrami and Doulati Ardejani, with the aim of predicting the pyrite oxidation rate fraction in the wastes of the Central Alborz coal washing pile in Iran, have presented a hybrid method, coupling simulated annealing and artificial neural networks. Because this designed ANN/SA model could enable the system to escape local minima, it was able to estimate the fraction of pyrite remaining in the wastes strongly better than simple ANNs and multivariable least squares regression models.[38]

Utilizing fuzzy logic (FL) within ANN is an approach firstly introduced by Zadeh[39] with the aim to overcome the mentioned problems. In this theory, every object is indicated by membership functions (MFs) and is then assigned a degree, which is between 0 and 1.[40,41] One of the most problematic challenges of FL approach is obtaining its optimal parameters, ie, number and location of MFs and compositions of fuzzy rules. Adaptive neuro-fuzzy interference system, which was initially introduced by Jang,[42,43] is a new approach established by combining FL with ANN with the aim of making a better decision as well as minimizing the error. Adaptive neuro-fuzzy interference system reconstructs neural networks as hybrid intelligent systems by incorporating FL into neural networks to find the relationship between input and output data sets.[44] Neural networks can easily learn from the data. However, it is difficult to interpret the knowledge acquired by them, since the learning associated with each neuron and each weight is fairly complex to comprehend. Moreover, determining the optimum number for neurons in each layer and the optimum structure for the network and also the understanding of the physics of the problem concerning neural networks are very challenging. It should also be noted that in some problems, network parameters tend not to converge. The size of the data set used for training the network significantly controls the accuracy of the final results. In addition, it is quite difficult to predict (generalize) the performance of the network.[45] In contrast, FL cannot learn from the data by itself. Nonetheless, fuzzy-based models are easily understood as they use linguistic terms and the structure of IF-THEN rules rather than using numeric terms.[43] Similar to the previous methods, ANFIS has some parameters such as number of MFs and the learning rate,[46] which have to be optimized carefully. Also, the convergence rate for ANFIS trained with classic optimization methods is slow.[45] In this work, one of the most powerful optimization algorithms, ie, particle swarm optimization, was used to make ANFIS a powerful tool for simulating and predicting various processes such as application of biphasic nano-TiO_2 on β-naphthol photodegradation.

3.1 | Particle swarm optimization

Particle swarm optimization is a global optimization technique, which was first proposed by Kennedy and

Eberhart[47] in 1995. Exploring the behavior of swarms like swarm of insects was the inspiration behind this concept. Particle swarm optimization operates by starting with a crowd of particles and subsequently exploring for an optimum condition by performing population modification. Every particle travels with an adjustable velocity within a defined surface called cost surface. In this method, the velocity and position of each particle are iteratively updated with the aim of minimizing an objective function, by the following equations:

$$v_i^{n+1} = \omega v_i^n + c_1 r_1^n \left(x_{iLb}^n - x_i^n\right) + c_2 r_2^n \left(x_{gb}^n - x_i^n\right) \quad (2)$$

$$x_i^{n+1} = x_i^n + v_i^{n+1}, \quad (3)$$

where n stands for the number of iterations; v represents the velocity of each particle (i); x denotes the position of the particle, ω, which was developed to better control exploration and exploitation,[48] is the inertia weight; x_{iLb} signifies the best local position of particle (i); x_{gb} is the best global position obtained by each particle in the swarm; c_1 and c_2 are the acceleration factors related to x_{iLb} and x_{gb}, respectively, and are typically set to 2; and r_1 and r_2 represent random values and are in the range of [0 1].

In the PSO method, the velocity vector of each particle is altered and this updated vector is then applied to the position of that particle. This velocity modification is subjected to the best local route and the best global route corresponding to the final minimum cost ever found by each particle in the swarm. If the cost of the best local candidate route is less than that of the existing best global route, the best global route will accordingly be substituted by the best local route. Subsequently, the velocity and the position of each particle are updated by using Equations 2 and 3.

3.2 | Artificial neural network trained with PSO

As mentioned earlier, one of the most problematic aspects of using ANN is assignment of the weights to design the network structure. To optimize the mentioned weights, PSO can be applied to train the ANN. This optimization is in the direction of minimizing the cost function. Mean squared error function is typically selected as the cost function. In the process of training a neural network, every particle indicates a vector of weights and biases. It is then inferred that in this approach, dissimilar from using common optimization algorithms such as BP, weights and biases are changed without executing any gradient. Indeed, if there is no gradient accessible for activation functions used in the ANN structure, an algorithm that depends only on gradient information cannot be used. In this case, weights are not adjusted per training iteration. Particle swarm optimization is used with the aim to minimize the cost function, which is achieved by updating weights and biases using Equations 2 and 3. Figure 2 schematically shows the use of PSO for training ANN.

3.3 | Execution of ANFIS training using PSO

The major challenge in modeling fuzzy logic is determination of the parameters of the fuzzy MFs. Given that these parameters are used by trial and error, another computational technique, eg, ANNS, can be combined with FL approach, which creates a new tool called "ANFIS." The purpose of ANFIS is to automate the determination process of the parameters and then minimize the error. While ANFIS is used for finding the relationship between input and output data in this work, there are yet some nonoptimal parameters because of the fact that ANN is being used. Even though ANN has a powerful learning algorithm, which can be used for finding FL's optimal parameters, both ANN and FL still have some nonoptimal parameters that can indirectly affect the performance of this intelligent tool. To overcome this challenge, PSO as a new and powerful algorithm is used in this work to find the optimal number of MFs and the best values for learning rate, Figure 3. This novel tool is applied on a case study (modeling and prediction of the application of biphasic nano-TiO_2 on β-naphthol photodegradation), and the results are subsequently compared with ANN-PSO. Then, by comparing the actual data (experimental results) with the prediction data (modeling results) obtained by the aforementioned approaches, the reliability of these novel tools is evaluated.

4 | DATA PREPARATION

Normalization of the data before the beginning of the modeling is typically suitable, since it helps to obtain a finer prediction by noise reduction. In this study, among various methods used for normalization, the following equation was used for normalizing input and output data. By using the minimum and maximum values of the dataset, this equation normalizes data in the range of [-1 1].

$$XN = \frac{X\text{-}MinX}{MaxX\text{-}MinX} \times 2\text{-}1, \quad (4)$$

where XN represents the data point targeted to be normalized and MinX and MaxX are respectively the minimum and maximum values of the dataset.

Using dependable experimental datasets is essential for constructing a reliable network. In this study, a total of 576 data points were applied to simulate the application of biphasic nano-TiO_2 on β-naphthol photodegradation. For this

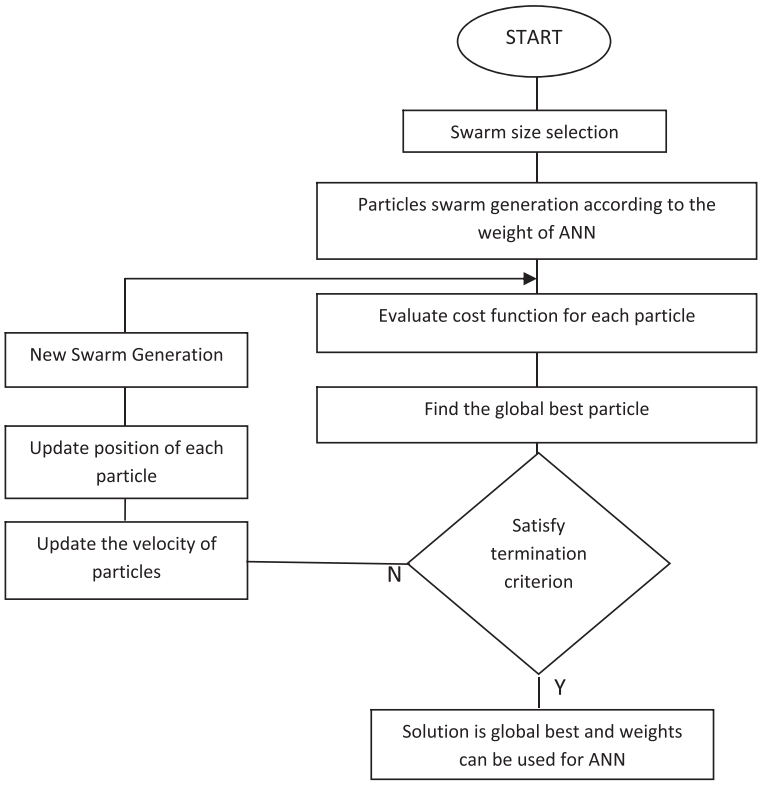

FIGURE 2 The flow chart for artificial network trained with particle swarm optimization (ANN-PSO) procedure

prediction, the data obtained from experimental works, which are input into the network are catalyst loading, beta-naphthol concentration, acidity, and aeration rate, while the amount of beta-naphthol photodegraded is the output. The data available for both ANN-PSO and ANFIS-PSO were categorized into 2 subsets. Four hundred sixty-one data points (approximately 80% of the original dataset) were used as the training set and the remaining 115 data points (nearly 20% of the original dataset) as the testing set. To demonstrate the proposed tools' performance in prediction of applying biphasic nano-TiO_2 on β-naphthol photodegradation, the data points in the testing set were not used throughout the training process. It should be noted the same training and testing data points were used for both ANN-PSO and ANFIS-PSO methods to obtain an accurate comparison of both tools. Applying FL to ANN-PSO is all the difference between these 2 methods. When ANN is combined with FL and PSO, given that the proposed approach automatically controls the parameters, the model is not required to be corrected manually.

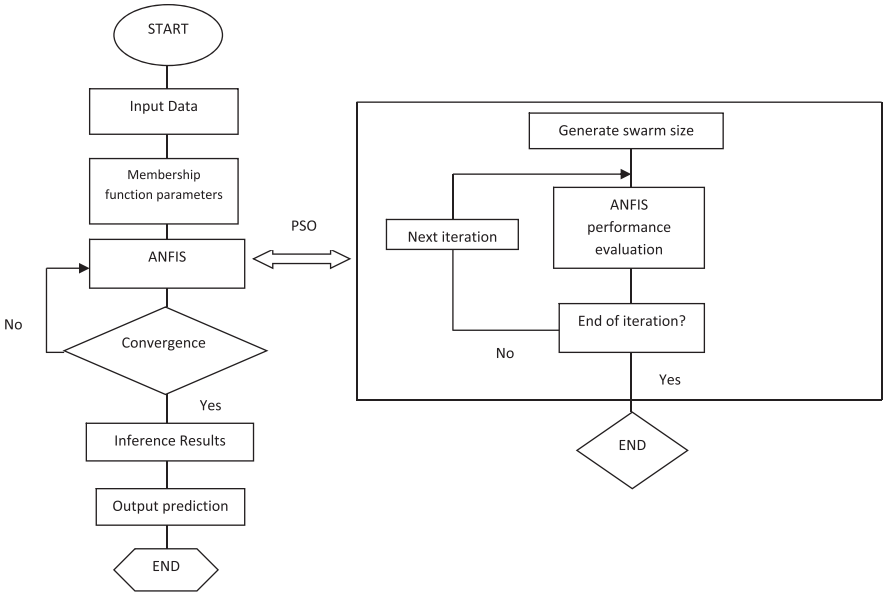

FIGURE 3 The flow chart for adaptive neuro-fuzzy interference system trained with particle swarm optimization (ANFIS-PSO) procedure

5 | RESULTS AND DISCUSSION

As previously mentioned, 2 methods are used for estimating the nonlinear relationship between the input and output variables. In this work, 576 data points obtained from different experiments were used for simulation of the application of biphasic nano-TiO_2 on β-naphthol photodegradation. Four hundred sixty-one data points were used as training data, while the remaining 115 data points were denoted as the testing data (unseen data).

When constructing a network by ANN, determination of the number of hidden layers and the number of neurons in each layer is of great importance. It is due to the fact that there is no reliable approach to specify these parameters. On the one hand, if too few hidden neurons are used, the ability of the network for modeling different processes will be undermined; and on the other, if too many hidden neurons are used, the network will be inadequately generalized for the unseen data. In this work, some configurations such as 5-x-1, 10-x-1, 15-x-1 and 20-x-1 are chosen, that 15-x-1 gave the minimum Mean Squared Error (MSE). So 15-x-1 is used to find hidden layer (x). Different 15-x-1 configurations were used to find the optimal network constructed with ANN-PSO. As demonstrated by the results, a network containing 11 neurons in its hidden layer (x) is the best configuration as it produced the minimum MSE, Figure 4. Table 1 shows the details of ANN, which was trained with PSO algorithm with the aim of predicting the application of biphasic nano-TiO_2 on β-naphthol photodegradation. It is known that the outputs of each layer are obtained by applying a transfer function to the weighted inputs. In the present study, hyperbolic tangent sigmoid transfer function (tansig) and linear transfer function (purelin) were respectively used in the hidden layers and the output layer. While tansig, an S-shaped function, which gives the outputs in the span of −1 to +1, is usually used in the hidden layers, purelin is often used in the output layer and produces the outputs in the range of $-\infty$ to $+\infty$. The definitions for hyperbolic tangent sigmoid transfer function (tansig) and linear transfer function (purelin) are presented in Equations 5 and 6, respectively.

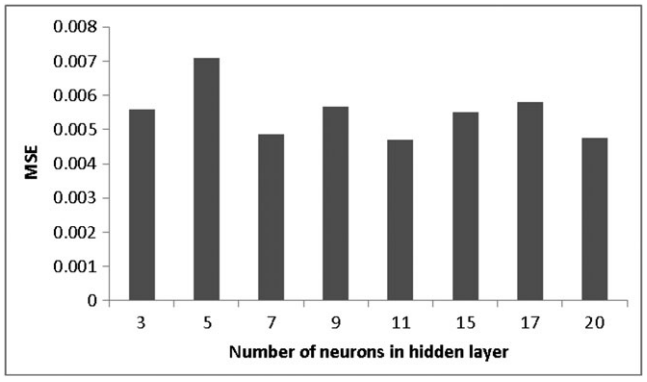

FIGURE 4 Mean squared error (MSE) variation with the number of neurons in the hidden layer

TABLE 1 Scenario used for adapting the artificial neural network with particle swarm optimization training variables

Type	Value
Input layer	15 neurons
Hidden layer	11 neurons
Output layer	1 neuron
Activation function used for input and hidden layers	Tansig
Activation function used for output layer	Purelin
Max iteration	300
c1 and c2 used in Equation 2	2.0
The inertia weight used in Equation 2	1.0
Number of swarm particles	200

$$\text{tansig}(n) = \frac{2}{1+e^{-2n}} - 1 \quad (5)$$

$$\text{purelin}(n) = n, \quad (6)$$

where, n represents the net input signal.

For an accurate comparison of different methods, same as ANN-PSO, ANFIS-PSO was also used with the same training and testing data, which were used for ANN-PSO. In comparison with ANN-PSO, ANFIS-PSO is more efficient for prediction. This supremacy, which is due to the virtue of ANFIS in eliminating local minima, yet is lacking in the design of ANN, was illustrated by comparing the statistical parameters used for assessing the performance of the 2 approaches, ie, average relative error (ARE), MSE, and R^2. The results shown in the figures and tables included in this paper also support the fact that ANFIS-PSO was a more accurate method to predict beta-naphthol degradation than was ANN-PSO. In this approach, MSE is selected as the fitness function, which is used as a standard for achieving the best result. To find the parameters, which are most suitable for the network, several networks were trained. Particle swarm optimization causes the network to converge on the best structure, and accordingly, a structure having 3 nodes in the MFs layer was obtained. Determining the type of MF most suitable for training the network is the major challenge of using ANFIS-PSO. The best MF was acquired according to the obtained ARE for both training and testing data sets, Table 2. Average relative error is defined as follows:

$$\text{Average Relative Error(ARE)} = \frac{\sum_{i=1}^{N} \left| y_i^{sim} - y_i^{ac} \right| / y_i^{ac}}{N}, \quad (7)$$

where N represents the number of data points, y_i^{ac} denotes

TABLE 2 Comparison between different membership functions used in ANFIS-PSO structure

Type of MF	Training data (%ARE)	Test data (%ARE)	Overall ARE (%)
trimf	2.4	6.4	3.20
trapmf	1.84	5.84	2.64
gbelmf	1.85	5.39	2.57
gaussmf	1.91	4.83	2.50
gauss2mf	1.89	11.3	3.77
pimf	1.82	4.9	2.43
dsigmf	1.82	5.05	2.46
psigmf	1.82	5.05	2.46

Abbreviations: ANFIS-PSO, adaptive neuro-fuzzy interference system trained with particle swarm optimization; ARE, average relative error; MF, membership function.

the experimental (actual) data point at the sampling data, and y_i^{sim} stands for the simulated data point or the output of the correlation.

As can be seen in Table 2, compared with other MFs, Π-shaped built-in membership function (pimf) produces the least ARE. This type of MF is defined as follows:

$$f(x;a,b,c,d)=\begin{cases}0 & x \pounds a\\ 2\left(\frac{x-a}{b-a}\right)^2 & a \pounds x \pounds \frac{a+b}{2}\\ 1-2\left(\frac{x-b}{b-a}\right)^2 & \frac{a+b}{2} \pounds x \pounds b\\ 1 & b \pounds x \pounds c\\ 1-2\left(\frac{x-c}{d-c}\right)^2 & c \pounds x \pounds \frac{c+d}{2}\\ 2\left(\frac{x-d}{d-c}\right)^2 & \frac{c+d}{2} \pounds x \pounds d\\ 0 & x^3 d\end{cases}. \quad (8)$$

The parameters a and d represent the "feet" of the curve, while c and d denote its "shoulders." The MF is assessed at the points given by the vector x.

Correlation coefficient (R^2) is another statistical criterion used for specifying the performance and integrity of the evolved smart intelligent approaches in prediction of the

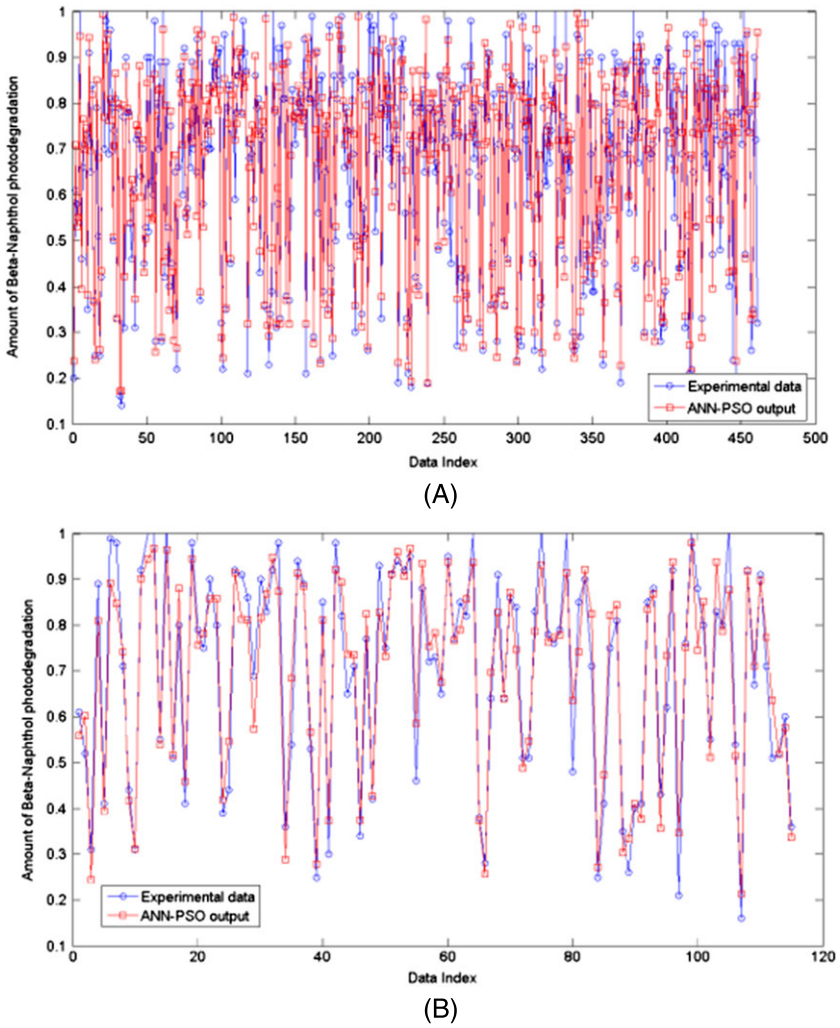

FIGURE 5 Performance of artificial network trained with particle swarm optimization (ANN-PSO) method in predicting the amount of β-naphthol photodegradation. A, Training data; B, testing data

target. The definition of this parameter is as follows:

$$\text{Correlation Coefficient}\left(R^2\right) = 1 - \frac{\sum_{i=1}^{N}\left(y_i^{ac} - y_i^{sim}\right)^2}{\sum_{i=1}^{N}\left(y_i^{ac} - y^{\overline{ac}}\right)^2}. \quad (9)$$

y^{ac} is the average of the experimental (actual) data.

Figures 5 and 6 illustrate the predicted and actual data points of the amount of β-naphthol photodegradation at stages of training and testing for both ANN-PSO and ANFIS-PSO methods, respectively. As can be seen from the 2 figures, the simulated results of ANN-PSO are not as accurate as those of ANFIS-PSO and, as such, ANFIS-PSO approach displays higher accuracy than ANN-PSO does, Figure 6.

To present the results of both ANN-PSO and ANFIS-PSO approaches, regression graphs are plotted, which are shown in Figures 7 and 8, for ANN-PSO and ANFIS-PSO, respectively. These plots display the results with respect to the actual data. In these figures, the dashed line represents the best linear fitted line between the actual and predicted results, while the solid line shows the line of experimental values = simulation outputs or Y = X. As can be seen in Figures 7 and 8, ANFIS-PSO yields simulated results with higher accuracy than ANN-PSO does. Whereas ANN-PSO approach overestimates the results at the lower boundary of β-naphthol photodegradation, ANFIS-PSO adequately tracks the experimental values for the training and testing data. The difference in the results yielded by these methods can certainly be attributed to applying FL to ANN-PSO, which transforms it to a powerful tool for predicting and simulating numerous types of processes.

Equations 10 and 11 present the generated equations for the best linear fitted line for the training data assortment for ANN-PSO and ANFIS-PSO methods, respectively:

$$y = 0.91x + 0.071 \quad , \quad R^2 = 0.906 \quad (10)$$

$$y = x + 4.7\times10^{-17} \quad , \quad R^2 = 0.9959. \quad (11)$$

As can be seen from Equation 11, the correlation factor for the training data yielded by ANFIS-PSO is 0.9959, which

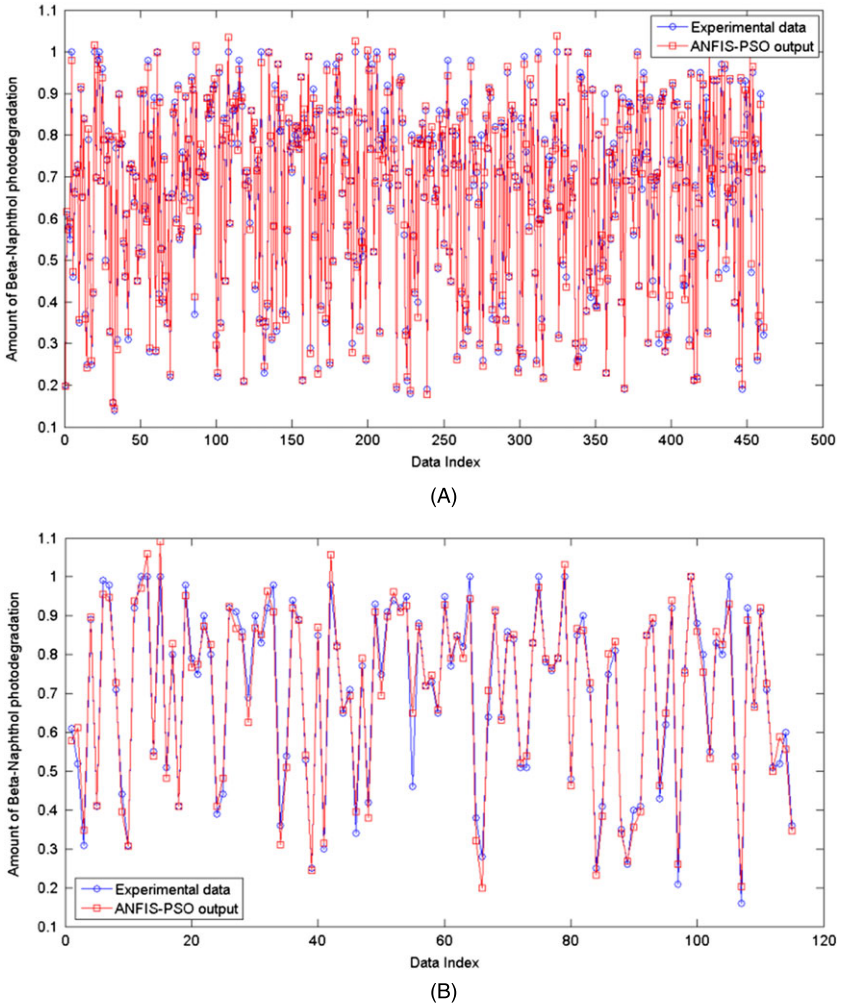

FIGURE 6 Performance of adaptive neuro-fuzzy interference system trained with particle swarm optimization (ANFIS-PSO) method in predicting the amount of β-naphthol photodegradation. A, Training data; B, testing data

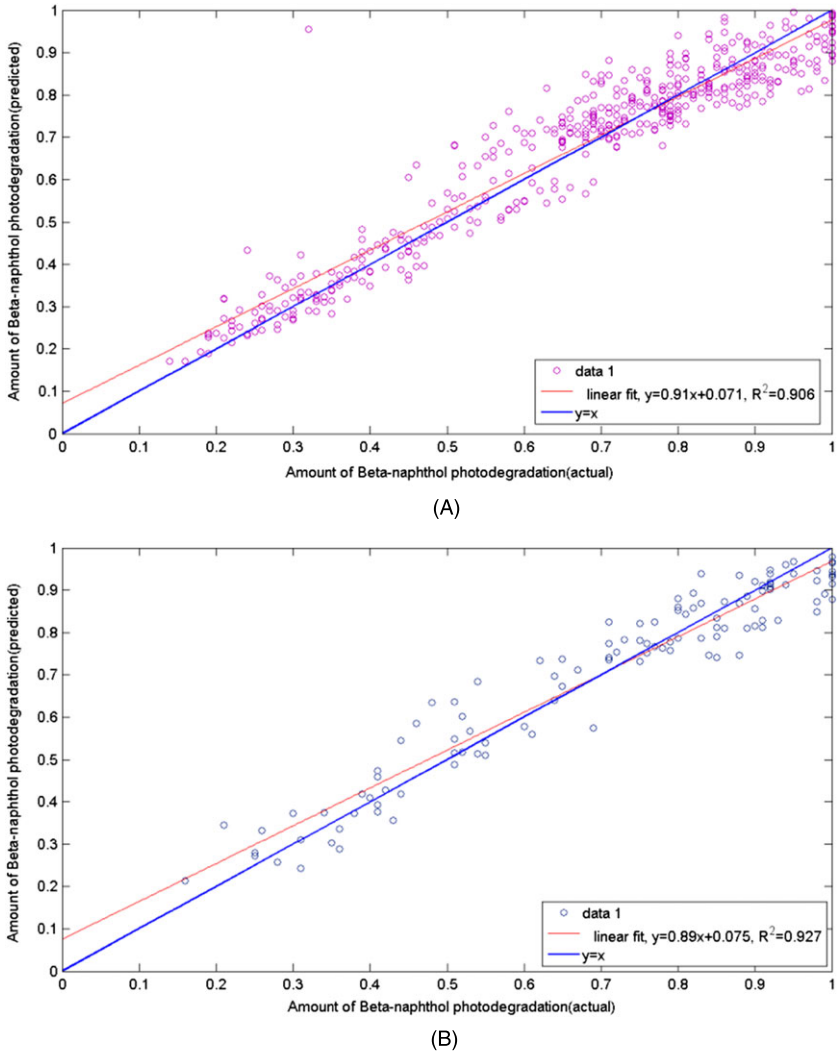

FIGURE 7 Regression plots for simulating β-naphthol photodegradation using artificial network trained with particle swarm optimization (ANN-PSO) approach. A, Training data; B, testing data

proves a very good correlation. Such high value for correlation factor signifies that the fitted line overlays with the diagonal line, y = x, as shown in Figure 7. This indicates that ANFIS-PSO approach can approximate and correlate the relationship between the input and output data at a very high accuracy.

The generated equations for the best linear fitted lines for the test data assortment yielded by ANN-PSO and ANFIS-PSO approaches are presented in Equations 12 and 13, respectively:

$$y = 0.89x + 0.075 \quad , \quad R^2 = 0.927 \tag{12}$$

$$y = 0.99x + 0.01 \quad , \quad R^2 = 0.973. \tag{13}$$

As was the case for the training data, the correlation factor of 0.973 obtained for test data for ANFIS-PSO results displays that the proposed ANFIS-PSO approach has the ability to estimate the actual values of β-naphthol photodegradation in different conditions at high integrity rate.

Figure 9 displays the percent deviation between the actual data and the predicted ones (outputs of models). The deviation (%) of ANN-PSO predicted outputs for both training and testing data are in the range of −198.28 to 21.7 with a minimum relative deviation of 0.044. While the percent deviation of ANFIS-PSO outputs lie in the range of −41.11 to 28.55 with a minimum relative deviation of 0.021. The superiority of ANFIS-PSO over the other approaches in predicting conductivity in different conditions is plainly shown in Figure 9.

$$\text{Deviation}(\%) = \frac{\text{actual value - predicted value}}{\text{actual value}} \times 100 \tag{14}$$

By evaluating ARE, MSE, and R^2 for the 2 proposed tools, the superior robustness of ANFIS-PSO for simulating

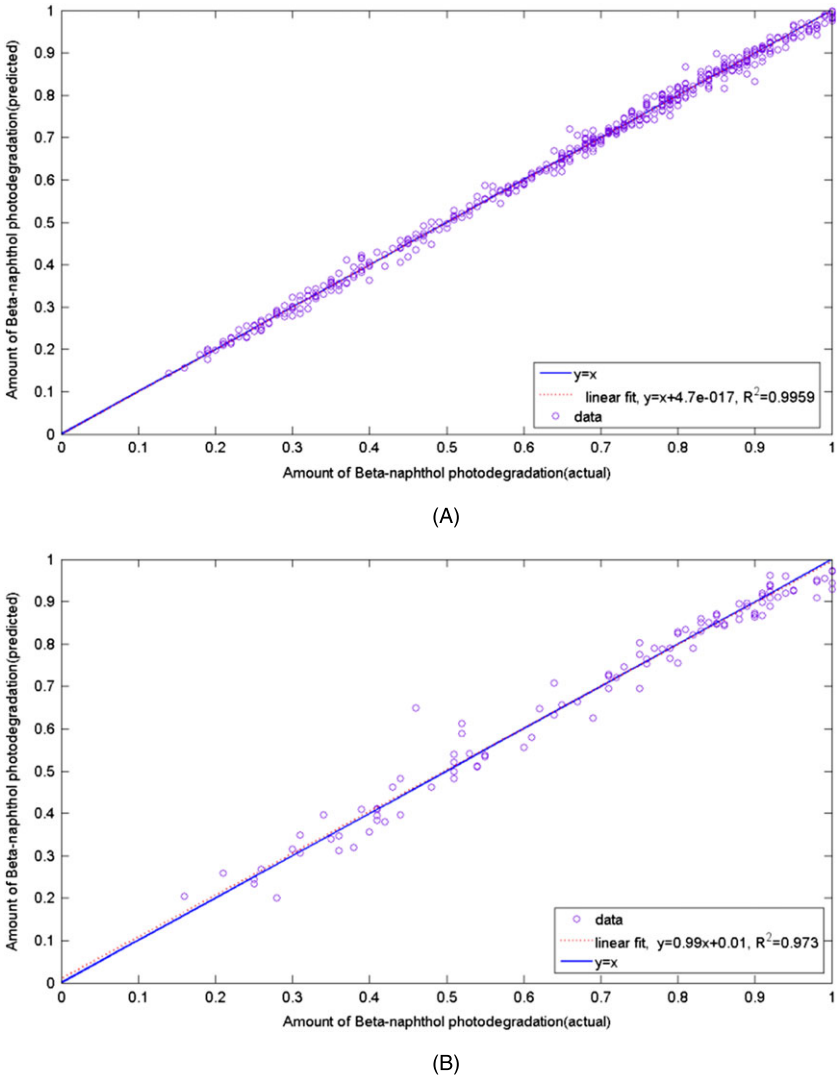

FIGURE 8 Regression plots for simulating β-naphthol photodegradation using adaptive neuro-fuzzy interference system trained with particle swarm optimization (ANFIS-PSO) approach. A, Training data; B, testing data

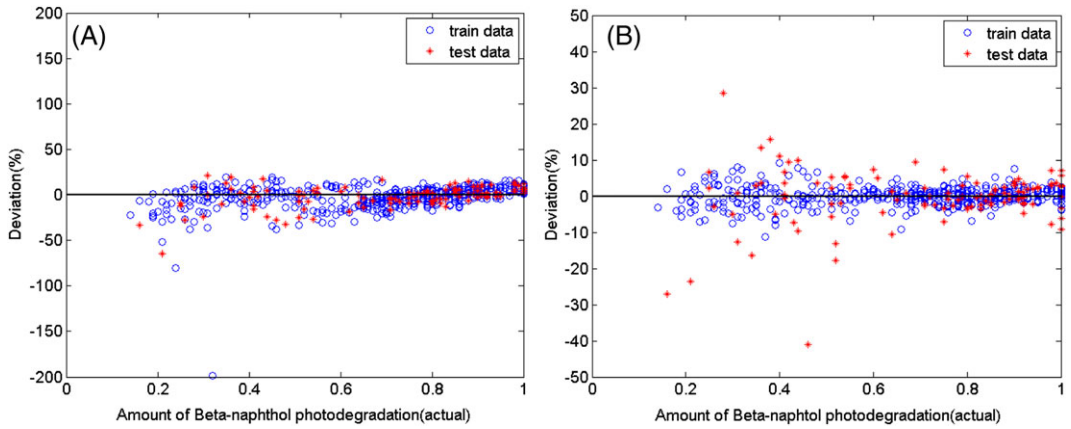

FIGURE 9 Deviation of predicted β-naphthol photodegradation using A, ANN-PSO method and B, ANFIS-PSO method

the application of biphasic nano-TiO_2 on β-naphthol photodegradation is firmly established, as presented in Table 3. By comparing the results yielded by these approaches for the training and testing data, it is concluded that the accuracy of ANFIS-PSO in modeling the mentioned process is higher than that of ANN-PSO.

TABLE 3 Comparison between the proposed methods for estimating β-naphthol photodegradation

	ANN-PSO			ANFIS-PSO		
	Train data	**Test data**	**Overall**	**Train data**	**Test data**	**Overall**
ARE (%)	8.83	8.45	8.75	1.82	4.9	2.43
MSE	0.0049	0.0039	0.0047	0.00021	0.0014	0.00045
R^2	0.906	0.927	0.91	0.9959	0.973	0.9913

Abbreviations: ANFIS-PSO, adaptive neuro-fuzzy interference system trained with particle swarm optimization; ANN-PSO, artificial network trained with particle swarm optimization; ARE, average relative error; MSE, mean squared error.

6 | CONCLUSION

In the present work, feasibility of using intelligent tools for prediction of photocatalytic degradation of beta-naphthol using the titanium dioxide (TiO_2) nanoparticles was investigated. For this purpose, a 3-layer feed forward neural network trained with particle swarm optimization algorithm and an ANFIS network trained with PSO were used for simulating this process. Factors affecting photocatalytic degradation of beta-naphthol, namely, impurity concentration, catalyst content, acidity, and aeration rate were designated as the input variables, while the amount of beta-naphthol photodegradation was taken as the output. Based on the results, ANFIS-PSO is a more efficient tool for prediction of photocatalytic behavior of TiO_2 nanoparticles for degradation of beta-naphthol in comparison with ANN-PSO. It is attributable to the advantageous ability of ANFIS in eliminating the local minima, which should be located in design of ANN. In predicting beta-naphthol photodegradation using all experimental data points, the ANFIS-PSO method accomplished a much low average relative error of 2.43%, and therefore, it can be a useful method as it is computationally simple to use along with high accuracy.

REFERENCES

1. Ameta R, Benjamin S, Ameta A, Ameta SC. Photocatalytic degradation of organic pollutants: a review. Paper presented at: Materials Science Forum; 2013.
2. Lazar MA, Varghese S, Nair SS. Photocatalytic water treatment by titanium dioxide: recent updates. *Catalysts* 2012;2(4):572-601.
3. Wang JB, Xu CH, Han WY, Zhu WP, Li YN. Photolytic and photocatalytic degradation of phenols in aqueous solution. Paper presented at: Advanced Materials Research; 2012.
4. Qourzal S, Barka N, Tamimi M, Assabbane A, Ait-Ichou Y. Photodegradation of 2-naphthol in water by artificial light illumination using TiO 2 photocatalyst: identification of intermediates and the reaction pathway. *Appl Catal Gen* 2008;334(1):386-393.
5. Gevrey M, Dimopoulos I, Lek S. Review and comparison of methods to study the contribution of variables in artificial neural network models. *Ecol Model* 2003;160(3):249-264.
6. Hippert HS, Pedreira CE, Souza RC. Neural networks for short-term load forecasting: a review and evaluation. *IEEE Trans Power Syst* 2001;16(1):44-55.
7. Arhami M, Kamali N, Rajabi MM. Predicting hourly air pollutant levels using artificial neural networks coupled with uncertainty analysis by Monte Carlo simulations. *Environ Sci Pollut Res* 2013;20(7):4777-4789.
8. Charisiadis P, Andra SS, Makris KC, et al. Spatial and seasonal variability of tap water disinfection by-products within distribution pipe networks. *Sci Total Environ* 2015;506:26-35.
9. Wen X, Fang J, Diao M, Zhang C. Artificial neural network modeling of dissolved oxygen in the Heihe River, Northwestern China. *Environ Monit Assess* 2013;185(5):4361-4371.
10. Jafar R, Shahrour I, Juran I. Application of artificial neural networks (ANN) to model the failure of urban water mains. *Math Comput Model* 2010;51(9):1170-1180.
11. Wu W, Dandy G, Maier H. Application of artificial neural networks to forecasting water quality in a chloraminated water distribution system. Paper presented at: 19th International Congress on Modeling and Simulation, Perth, Australia. http://mssanz.org.au/modsim2011; 2011.
12. Khataee AR, Kasiri MB. Modeling of biological water and wastewater treatment processes using artificial neural networks. *CLEAN–Soil, Air, Water* 2011;39(8):742-749.
13. Solaimany-Aminabad M, Maleki A, Hadi M. Application of artificial neural network (ANN) for the prediction of water treatment plant influent characteristics. *J Adv Environ Health Res* 2014;1(2):89-100.
14. Cho S, Lim B, Jung J, et al. Factors affecting algal blooms in a man-made lake and prediction using an artificial neural network. *Measurement* 2014;53:224-233.
15. Kia MB, Pirasteh S, Pradhan B, Mahmud AR, Sulaiman WNA, Moradi A. An artificial neural network model for flood simulation using GIS: Johor River Basin, Malaysia. *Environ Earth Sci* 2012;67(1):251-264.
16. Das L, Maity U, Basu JK. The photocatalytic degradation of carbamazepine and prediction by artificial neural networks. *Process Saf Environ Prot* 2014;92(6):888-895.
17. Eskandarloo H, Badiei A, Behnajady MA. Study of the effect of additives on the photocatalytic degradation of a triphenylmethane dye in the presence of immobilized TiO2/NiO nanoparticles: artificial neural network modeling. *Ind Eng Chem Res* 2014;53(17):6881-6895.

18. Jing L, Chen B, Zhang B. Modeling of UV-induced photodegradation of naphthalene in marine oily wastewater by artificial neural networks. *Water Air Soil Pollut* 2014;225(4):1-14.
19. Mustafa YA, Jaid GM, Alwared AI, Ebrahim M. The use of artificial neural network (ANN) for the prediction and simulation of oil degradation in wastewater by AOP. *Environ Sci Pollut Res* 2014;21(12):7530-7537.
20. Sabonian M, Behnajady MA. Artificial neural network modeling of Cr (VI) photocatalytic reduction with TiO2-P25 nanoparticles using the results obtained from response surface methodology optimization. *Desalin Water Treat* 2015;56(11):2906-2916.
21. Ijadpanah-Saravy H, Safari M, Khodadadi-Darban A, Rezaei A. Synthesis of titanium dioxide nanoparticles for photocatalytic degradation of cyanide in wastewater. *Anal Lett* 2014;47(10):1772-1782.
22. Ijadpanah-Saravi H, Dehestaniathar S, Khodadadi A, Safari M. Optimization of photocatalytic degradation of β-naphthol using nano TiO2-activated carbon composite. *Desalin Water Treat* 2016;57(10):4708-4719.
23. Iwaszuk A, Mulheran PA, Nolan M. TiO 2 nanocluster modified-rutile TiO 2 photocatalyst: a first principles investigation. *J Mater Chem A* 2013;1(7):2515-2525.
24. Ding Z, Zhu H, Lu G, Greenfield P. Photocatalytic properties of titania pillared clays by different drying methods. *J Colloid Interface Sci* 1999;209(1):193-199.
25. Bose NK. *Neural Network Fundamentals with Graphs, Algorithms, and Applications.* New York City: McGraw-Hill Education; 1996.
26. Hornik K, Stinchcombe M, White H. Multilayer feedforward networks are universal approximators. *Neural Netw* 1989;2(5):359-366.
27. Yamazaki A, De Souto M, Ludermir T. Optimization of neural network weights and architectures for odor recognition using simulated annealing. Paper presented at: Proceedings International Joint Conference on Neural Networks; 2002.
28. Lin M-L, Chen C-W. Application of fuzzy models for the monitoring of ecologically sensitive ecosystems in a dynamic semi-arid landscape from satellite imagery. *Eng Comput* 2010;27(1):5-19.
29. Wu X, Zhou Y. Reserve estimation using neural network techniques. *Comput Geosci* 1993;19(4):567-575.
30. Singer DA. Typing mineral deposits using their associated rocks, grades and tonnages using a probabilistic neural network. *Math Geol* 2006;38(4):465-474.
31. Mahmoudabadi H, Izadi M, Menhaj MB. A hybrid method for grade estimation using genetic algorithm and neural networks. *Comput Geosci* 2009;13(1):91-101.
32. Tahmasebi P, Hezarkhani A, Sahimi M. Multiple-point geostatistical modeling based on the cross-correlation functions. *Comput Geosci* 2012;16(3):779-797.
33. Weller AF, Harris AJ, Ware JA. Two supervised neural networks for classification of sedimentary organic matter images from palynological preparations. *Math Geol* 2007;39(7):657-671.
34. Daryasafar A, Ahadi A, Kharrat R. Modeling of steam distillation mechanism during steam injection process using artificial intelligence. *Scientific World Journal* 2014;2014:1-8.
35. Ghose T. Optimization technique and an introduction to genetic algorithms and simulated annealing. Paper presented at: Proceedings of International workshop on Soft Computing and Systems; 2002.
36. Samanta B, Bandopadhyay S, Ganguli R. Data segmentation and genetic algorithms for sparse data division in Nome placer gold grade estimation using neural network and geostatistics. *Explor Min Geol* 2002;11(1-4):69-76.
37. Yan F, Lin Z. New strategy for anchorage reliability assessment of GFRP bars to concrete using hybrid artificial neural network with genetic algorithm. *Compos Part B Eng* 2016;92:420-433.
38. Bahrami S, Ardejani FD. Prediction of pyrite oxidation in a coal washing waste pile using a hybrid method, coupling artificial neural networks and simulated annealing (ANN/SA). *J Clean Prod* 2016;137:1129-1137.
39. Zadeh LA. Fuzzy sets. *Inf Control* 1965;8(3):338-353.
40. Ghafoori M, Roostaeian M, Sajjadian V. A state-of-the-art permeability modeling using fuzzy logic in a heterogeneous carbonate: an Iranian carbonate reservoir case study. Paper presented at: International Petroleum Technology Conference; 2008.
41. Vasant P, Elamvazuthi I, Webb JF. Fuzzy technique for optimization of objective function with uncertain resource variables and technological coefficients. *Int J Model Simul Sci Comput* 2010;1(03):349-367.
42. Jang J-S. *Neuro-Fuzzy Modeling: Architectures, Analyses, and Applications*. Berkeley: University of California; 1992.
43. Jang J-S. ANFIS: adaptive-network-based fuzzy inference system. *IEEE Trans Syst Man Cybern* 1993;23(3):665-685.
44. Daryasafar A, Azad EG, Ghahfarokhi AK, Mousavi SF. Simulation studies on growth and death of microorganisms using the oil-degrading bacteria Petrotoga sp. *Chem Eng Technol* 2014;37(12):2152-2164.
45. Anemangely M, Ramezanzadeh A, Tokhmechi B. Shear wave travel time estimation from petrophysical logs using ANFIS-PSO algorithm: a case study from Ab-Teymour oilfield. *J Nat Gas Sci Eng* 2017; 373-387.
46. Shoorehdeli MA, Teshnehlab M, Sedigh A. Stable learning algorithm approaches for ANFIS as an identifier. *IFAC Proc Vol* 2008;41(2):7046-7051.
47. Kennedy J, Eberhart RC. Particle swarm optimization. Paper presented at: Proc IEEE Int Conf on Neural Networks; 1995.
48. Shi Y, Eberhart RC. Parameter selection in particle swarm optimization. Paper presented at: International Conference on Evolutionary Programming; 1998.

How to cite this article: Ijadpanah-Saravi H, Safari M, Noruzi-Masir B, Darban AK, Bakhshi P. Intelligent tools to model photocatalytic degradation of beta-naphtol by titanium dioxide nanoparticles. *Journal of Chemometrics*. 2017;e2907. https://doi.org/10.1002/cem.2907